Cell Reports, Volume *43*

Supplemental information

Distributed X chromosome inactivation in brain circuitry is associated with X-linked disease penetrance of behavior

Eric R. Szelenyi, Danielle Fisenne, Joseph E. Knox, Julie A. Harris, James A. Gornet, Ramesh Palaniswamy, Yongsoo Kim, Kannan Umadevi Venkataraju, and Pavel Osten

SUPPLEMENTAL INFORMATION
Supplemental Figures

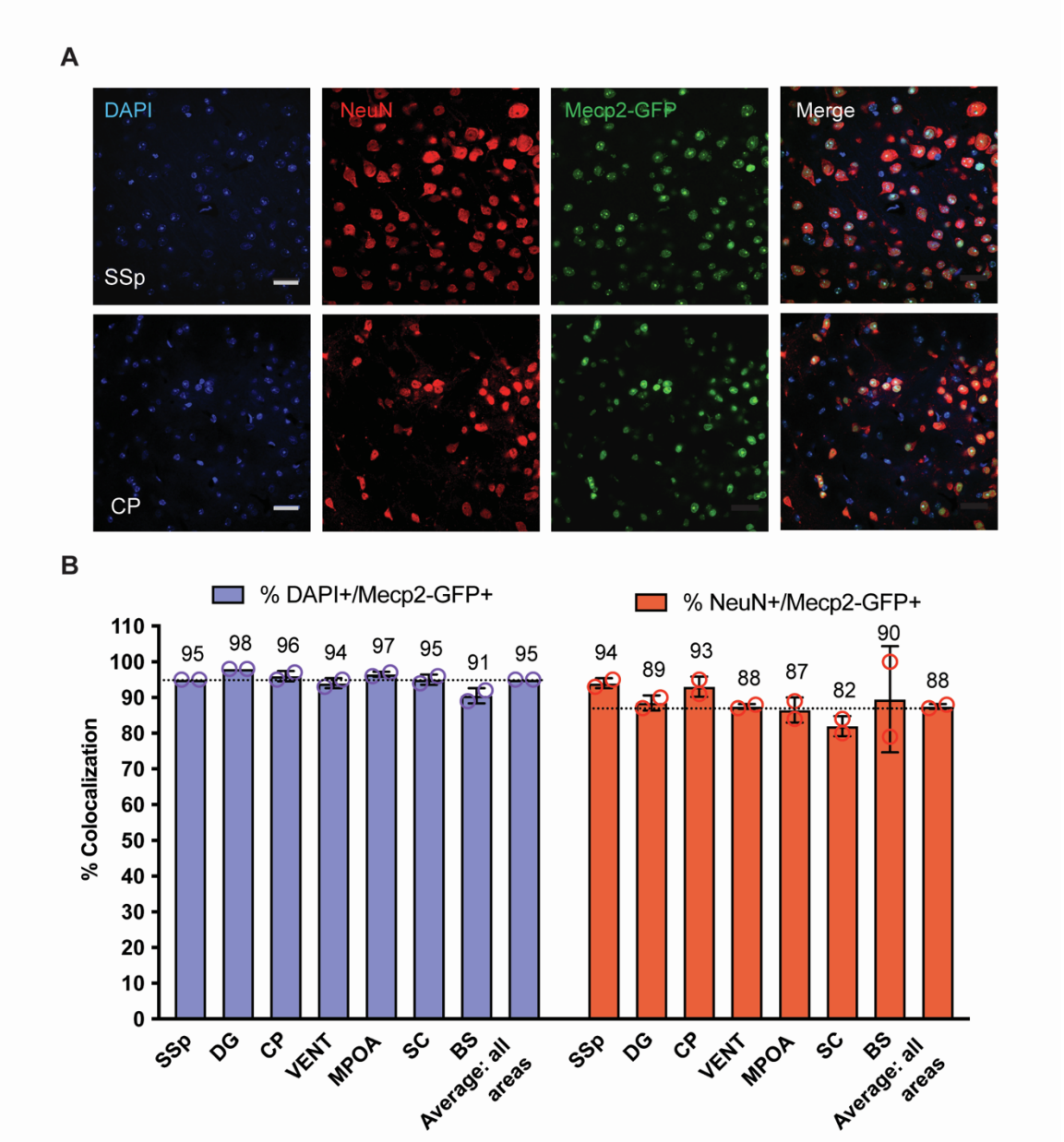

Figure S1: Cellular labeling performance of Mecp2-GFP X-reporter allele in homozygous Mecp2-GFP(m/p) brain, related to Fig. 1. A) Representative images of DAPI and NeuN counter-stained sections from somatosensory cortex (SSp) and caudate putamen (CP) areas in a homozygous Mecp2-GFP(m/p) brain (scale bar = 25 um). B) Quantification of DAPI and NeuN colocalization with Mecp2-GFP(m/p) expression across seven brain areas (mean ± SD).

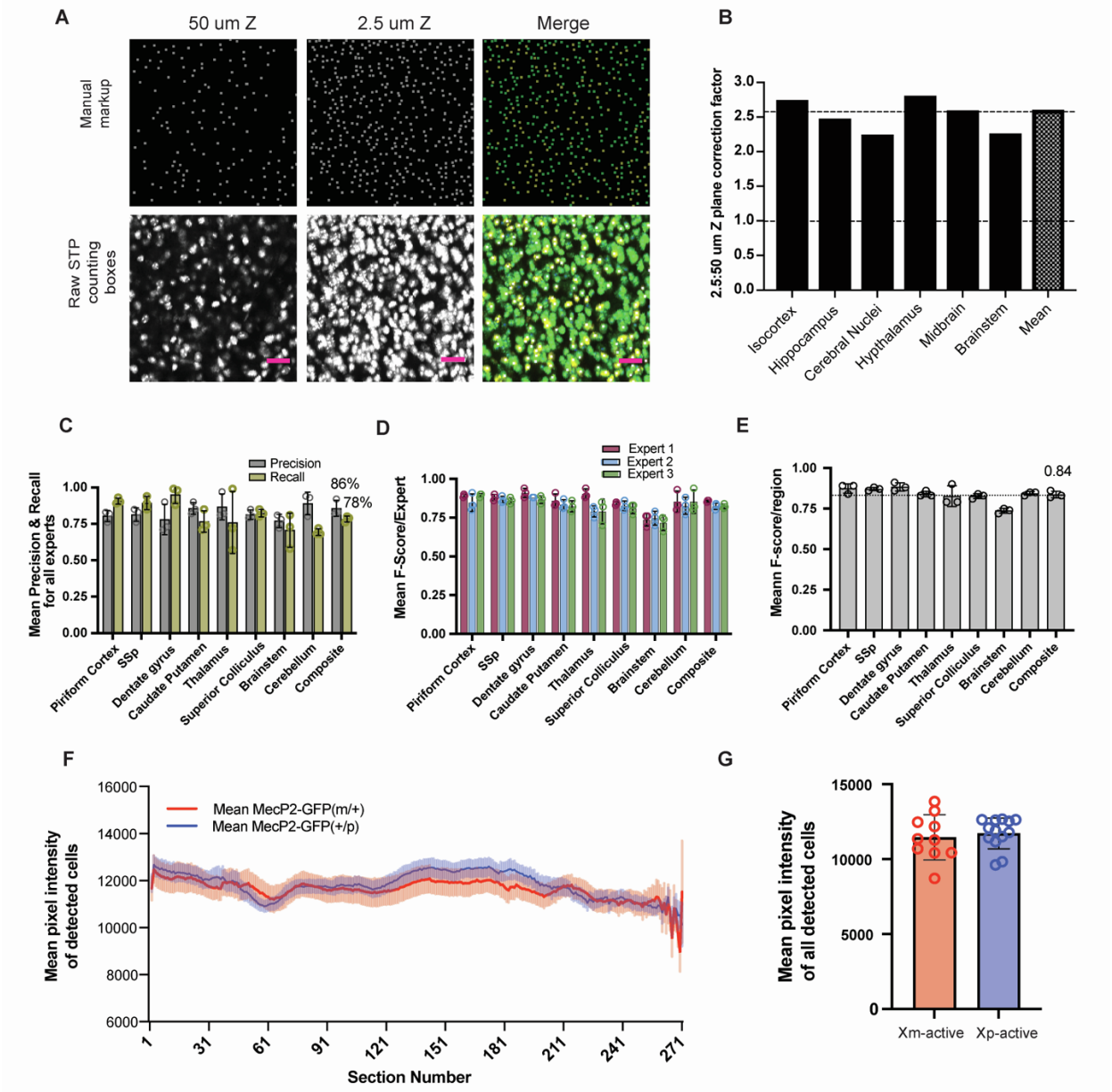

Figure S2: Validation and benchmarking of Mecp2-GFP+ cell detection related to Fig. 1-2. A-B) Data used to calculate a serial 2D to 3D cell count conversion factor. A**)** An example of a manual cell count markup (top row) and raw STPT image (bottom row) from a homozygous Mecp2-GFP(m/p) brain (ventromedial hypothalamus). Manual markup was made for a 3D brain volume imaged at a Z resolution of 2.5 μm. The 3D manual cell count was compared to a convolutional network (CN) based cell count from a single plane in the middle of the 3D stack. Scale bar = 25 um. B) 2D to 3D conversion factors were calculated by dividing the manual 3D cell counts by the single plane CN-based cell count for selected brain areas. The mean conversion factor of 2.6 was then used for all brain regions. C-E) F-score calculations of CN performance in detecting GFP+ cells based on expert ground truth data (see Methods). The calculations were performed on 8 select tiles from different brain regions covering a range of cell densities from 3 Mecp2-GFP(+/p)

brain samples. C) Mean CN precision and recall. D) Mean CN F-score derived from precision and recall values of (c) for each individual expert across regions. E) Mean CN F-score shown for all regions. F-G) Fluorescence intensity comparisons of Mecp2-GFP+ cell nuclei across genotypes (n=10, 12). F) Mean cellular pixel intensity from each section (270 sections total; anterior limit = 1; posterior limit = 270) of Xm-active (red) or Xp-active (blue) cells. G) Group comparison of mean pixel intensity across all segmented cells. All values = mean ± SEM.

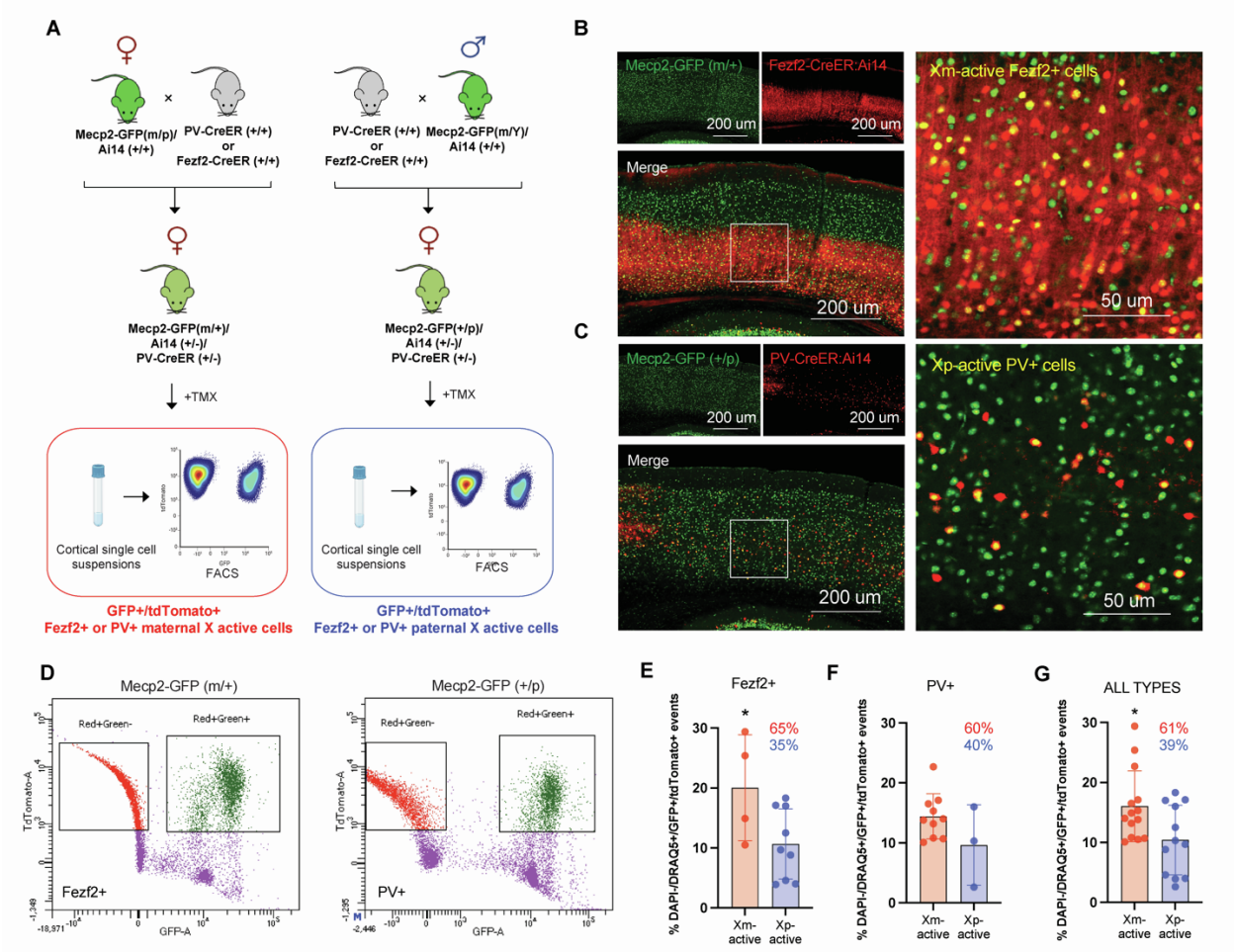

Figure S3: Validation of STPT cell counts with FACS in genetically defined cortical neurons related to Fig. 1. A) Breeding strategy to derive triple transgenic Mecp2-GFP (+/p or m/+)/Ai14/Cre-driver (Fezf2-CreER or Pv-CreER) mice. Tamoxifen was administered twice between P20-P30 to label defined cell-types, and unilateral live cortical dissociation and single cell suspensions were prepared for FACS sorting ~7 days later. B) Representative 2-channel STPT images in the primary motor cortex of a Mecp2-GFP (m/+)/Ai14/Fezf2-CreER mouse at two magnifications. C) Representative 2-channel STPT images in the primary motor cortex of a Mecp2-GFP (+/p)/Ai14/PV-CreER mouse at two magnifications. D) Representative final FACS gating of tdTomato+/EGFP- and EGFP/tdTomato+ cells for Fezf2-CreER (left) or PV-CreER (right) driver mice. E-G) Percent DAPI-/DRAQ5+/EGFP+/tdTomato+ events from parent gate for Mecp2-GFP(+/p) (Xm-active) and Mecp2-GFP(m/+) (Xp-active) cells across (E) Fezf2+ (n = 4, 9), and (F) PV (n = 10, 3), and (G) combined cell-types (n = 14, 12) (mean ± SD). Unpaired t test: $p < 0.05$, (F) Xm-active: Unpaired t test: $p = 0.131$ (G) Xm-active: Unpaired t test: $p = 0.22$. Each data point represents events derived from a unilateral cortex from 1 animal. Sum mean percent of Xm-active and Xp-active is displayed for each cell-type.

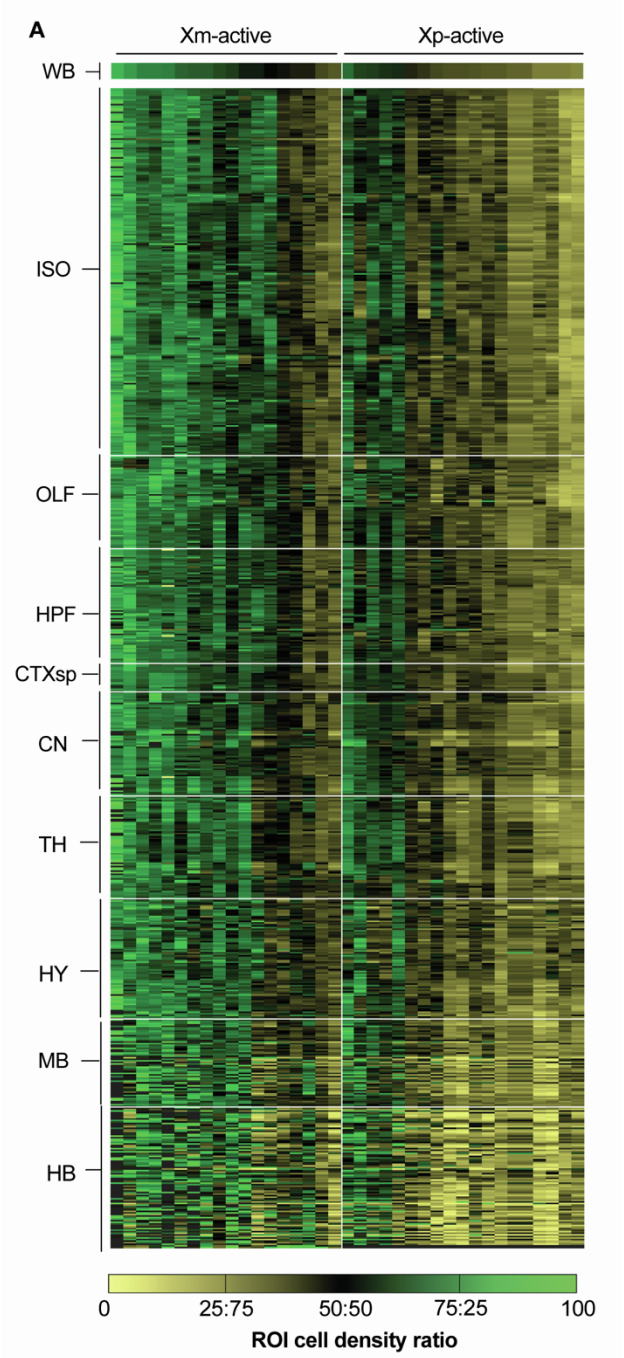

Figure S4: Quantification of stochastic Xm and Xp selection across all brain regions related to Fig. 1. A) 2D heatmap of brain-wide ROI cell density ratios in which each column represents one animal from maternal Mecp2-GFP(m/+) (left) and paternal Mecp2-GFP(p/+) (right) reporter brains. The Xm and Xp selection is expressed as measured:estimated cell density ratios across all 738 brain ROIs and displayed on a color gradient of beige to black (0 to 50:50), and black to green (50:50 to 100%). The samples are ordered from high (left) to low (right) XCI selection for each genetic group on the x-axis whereby the ROIs are ordered by major ontological division along the y-axis.

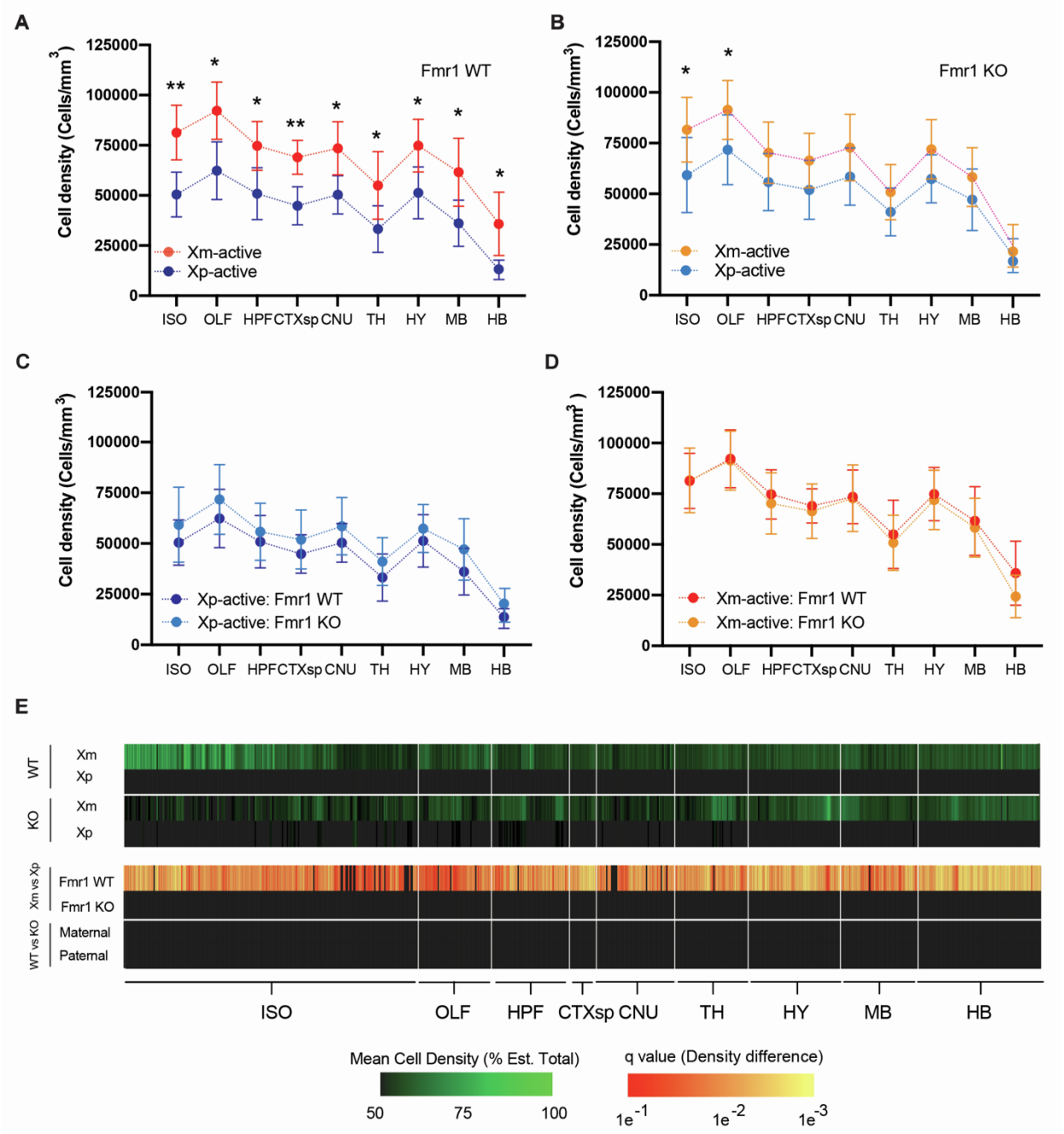

Figure S5: ROI-based healthy cell density analyses in Fmr1 WT and heterozygous KO mice related to Fig. 2. A-D) Healthy cell density (cells/mm^3; mean ± SD) comparisons amongst (A) Xm-active and Xp-active Fmr1 WT, (B) Xm-active and Xp-active Fmr1 KO, (C) Xp-active Fmr1 WT and KO, and (D) Xm-active Fmr1 WT and KO mice across major ontological divisions of the brain. Fmr1 WT (Xm-active (n=8), Xp-active (n=7) or heterozygous KO mice (Xm-active (n=7), Xp-active (n=8)) *p<0.05, **p<0.01, 2-way mixed effects ANOVA with Holm-Sidak multiple comparison correction. E) Brain-wide cell density comparisons in Fmr1 WT and heterozygous KO mice. Columns 1-4: Brain-wide heat map visualization of mean healthy Xm-active and Xp-active ROI cell densities (% of estimated total) on a color gradient of black (50%) to green (100%) amongst Fmr1

WT and KO mice. Columns 5-8: Brain-wide q values of ROI cell density statistical comparisons of active XC parent-of-origin amongst Fmr1 WT and Fmr1 KO mice (top), and cell density comparisons amongst mice with WT or KO Fmr1 alleles with matched active XC parent-of-origin (bottom). Legends indicating color scaling for mean cell density (left) and q values (right) are listed at the bottom.

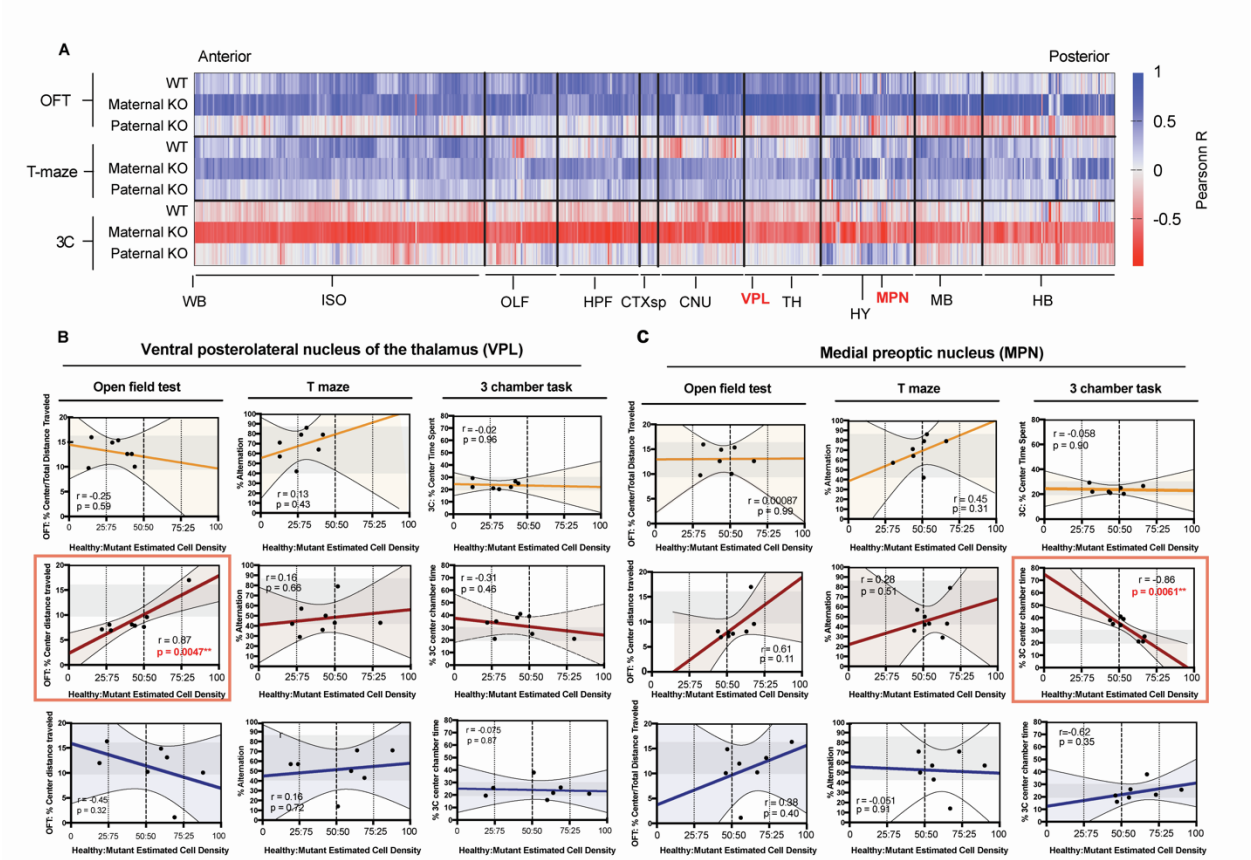

Figure S6: Raw Pearson r values and scatterplot examples across genetic groups and behavioral tests related to Fig. 3. A) 2D heat maps of raw Pearson correlation r values corresponding to across brain ROIs grouped by major ontological structures from anterior (left) to posterior (right) positions of the whole-brain. Raw Pearson r values are represented on a color gradient scale from -1 (red) to 0 (white) to 1 (blue). Results from Fmr1 WT ("WT"), maternal Fmr1-KO(m)/Mecp2-GFP(p) ("Maternal KO") and paternal Fmr1-KO(p)/Mecp2-GFP(m) ("Paternal KO") mice are grouped by each behavioral test: top: OFT, middle: T maze, bottom: 3-chamber (3C). B-C) Individual scatterplot visualization of the data from (A) for each behavioral group and behavioral test for the (B) ventral posterolateral nucleus of the thalamus (VPL), and (C) medial preoptic nucleus (MPN). Raw r and p values of statistical tests are inlayed within each panel. Red boxes bound correlations that reached statistical significance.

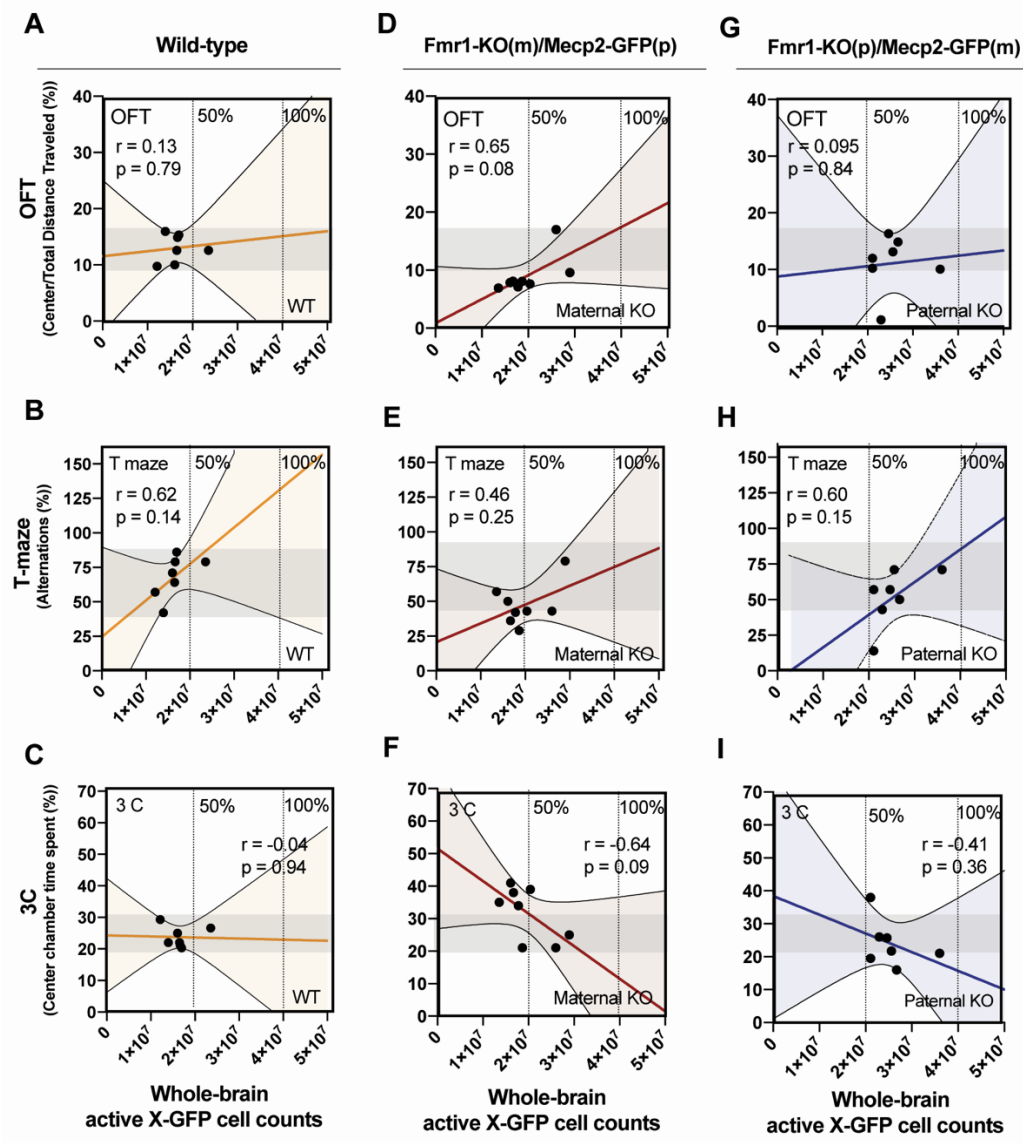

Figure S7: Whole-brain cell count correlations with behavior related to Fig. 3. (A-C; left) Fmr1 WT, (D-F; center) maternal Fmr1 KO, and (G-I; right) paternal Fmr1 KO whole-brain cell counts correlated to (A, D, G; top) OFT, (B, E, H; middle) T maze, and (C, F, I; bottom) 3 chamber behavioral scores. Dashed lines indicate estimated 50 and 100% cell counts. Gray transparent boxes inside plots indicate Fmr1 WT range of behavioral scores for comparison across mutant groups. r and p value statistics are listed in each panel.

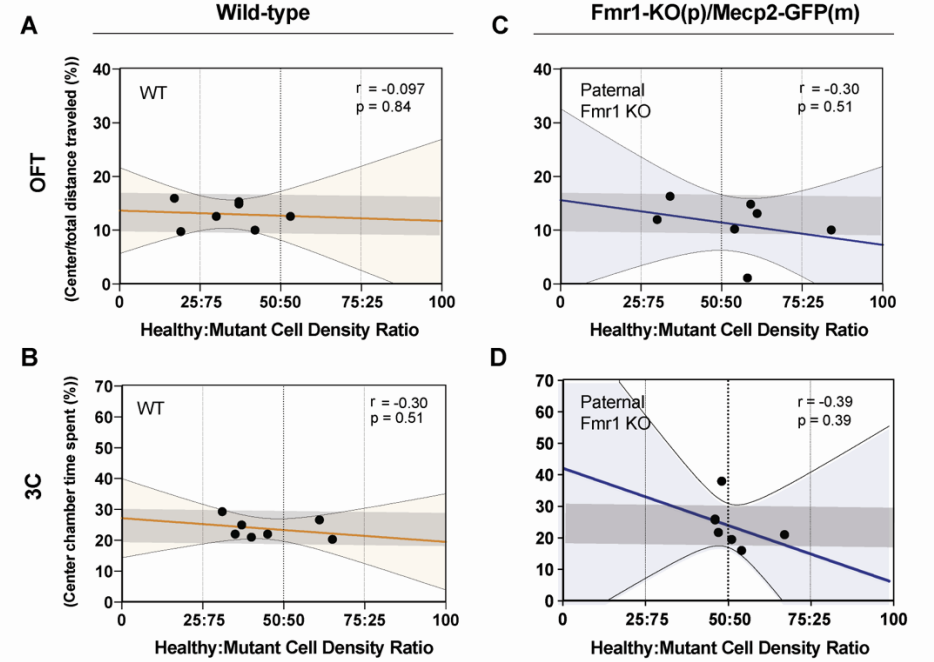

Figure S8: Control group correlations of behavioral circuit cell density ratios with behavioral scores related to Fig. 4. Fmr1 WT (A-B; left) and paternal Fmr1 KO (C-D; right) linear regression models of ROI network cell density ratios and scores from (A, C; top) OFT and (B, D; bottom) 3C behavioral assays. Regression and statistical test values are listed for each panel.

Supplemental Tables

Supplementary Table 1: Brain-wide descriptive statistics of cell counts, volumes, and cell densities related to **Fig. 1**

Supplementary Table 2: Brain-wide statistical results of Xm-active versus Xp-active cell density comparisons relate to **Fig. 1**

Supplementary Table 3: Brain-wide descriptive statistics of cell counts, volumes, and cell densities related to **Fig. 2**

Supplementary Table 4: Statistical results of brain-wide cell density comparisons in Fmr1 WT or heterozygous KO mice related to **Fig. 2**

Supplementary Table 5: Statistical results of brain-wide ROI cell density and behavioral score correlational screens related to **Fig. 3**

Supplementary Table 6: Normalized ROI connection density matrices related to **Fig. 4**

Supplementary Table 7: Structural circuitry of behaviorally correlated regions: raw data related to **Fig. 4**